

Diamond coatings for micro end mills: Enabling the dry machining of aluminum at the micro-scale

Patrick J. Heaney^a, Anirudha V. Sumant^{b,1}, Christopher D. Torres^c,
Robert W. Carpick^{b,2}, Frank E. Pfefferkorn^{c,*}

^a *Materials Science Program, University of Wisconsin-Madison, WI, 53706, United States*

^b *Department of Engineering Physics, University of Wisconsin-Madison, WI, 53706, United States*

^c *Department of Mechanical Engineering, University of Wisconsin-Madison, WI, 53706, United States*

Received 2 May 2007; received in revised form 26 November 2007; accepted 4 December 2007

Available online 8 December 2007

Abstract

We show that thin diamond coatings can dramatically enhance the performance of micrometer-scale cutting tools. We present a new approach for coating 300 μm diameter tungsten carbide (WC) micro end mills using a tailored seeding method and hot filament chemical vapor deposition (HFCVD) to obtain uniform, conformal, and continuous diamond coatings less than 2 μm in both thickness and grain size. The performance of the uncoated and coated tools has been evaluated by dry machining channels in 6061-T6 aluminum. The test results demonstrate far lower tool wear and breakage, much lower adhesion of aluminum to the tool, and significantly lower cutting forces for the coated tools. The coatings achieve a more predictable surface finish and enable dry machining at high speeds (40,000 rpm) with little or no burr formation. The improved performance of the coated tools is a result of the superior tribological properties of fine-grained diamond against aluminum, specifically low friction, low adhesion, and low wear of the film. Since the coating allows machining without lubricants and essentially eliminates metal burrs, this approach can reduce the environmental impact of micro-machining processes and offers greatly improved performance for micro and meso-scale manufacturing applications.

© 2007 Elsevier B.V. All rights reserved.

Keywords: Diamond film; Nanocrystalline; Hot filament CVD; Cutting tools

1. Introduction

Diamond has been emerging as an increasingly important material for a range of applications [1–3] due to beneficial physical and chemical properties such as a low coefficient of friction, high hardness, low wear rate, and chemical inertness. Diamond coatings are used for many components since these excellent properties are primarily required at the surface of a component, where it encounters a harsh environment. Chemical vapor deposition (CVD) enables the growth of polycrystalline diamond coatings on many substrates [1–6]. Polycrystalline

diamond is classified as micro-, nano-, or ultra-nano-crystalline if the average grain size is greater than 1–100 μm , 10–100 nm, or 2–10 nm, respectively. The properties of these coatings are to varying degrees similar to single crystal diamond [1,4].

Diamond coatings are commonly used to increase the performance of cutting tools [1–7]. These coatings significantly increase the performance of conventional (macroscopic) size cutting tools for a variety of reasons: (1) extremely high hardness (80–100 GPa), which helps reduce tool wear [1–7]; (2) low coefficients of friction against various workpiece materials (0.04–0.1), which decreases cutting and thrust forces and also reduces heat production [1–6]; (3) chemical inertness and low adhesion to most workpiece materials, which prevents built-up-edge (the build up of workpiece material on the tool rake face), dead-metal zones, and clogging of flutes [1–6].

Micro-manufacturing, the process of creating features measured in micrometers [8,9], is a rapidly growing worldwide

* Corresponding author. Tel.: +1 608 263 2668.

E-mail address: pfefferk@engr.wisc.edu (F.E. Pfefferkorn).

¹ Now at the Center for Nanoscale Materials, Argonne National Laboratory, Argonne, IL, United States.

² Now at the Dept. of Mechanical Engineering & Applied Mechanics, University of Pennsylvania, Philadelphia, PA, United States.

industry [10]. It is used, for example, in the miniaturization of common devices including actuators, motors, fuel cells, and gas turbines, and the production of packaging that links smaller devices, such as MEMS, to the macroscopic world. As technology shrinks and the demand for smaller devices grows, the ability to precisely shape new and existing materials at small scales becomes increasingly more important [8–10].

One particular micro-manufacturing process of growing importance is micro end milling. As the direct scale down of macroscopic milling, micro end milling (Fig. 1) is a material removal process that can generate three-dimensional features in a single step [7,9,10]. It does not require multiple process steps or a clean room environment, and can be used to manufacture components out of a wide variety of materials beyond silicon-based compounds [9,11,12]. Polymers [13], metals and metal alloys [14–20], and pre-sintered powder ceramics [21] have been successfully machined by micro end milling. This has enabled the manufacture of precision biomedical components,

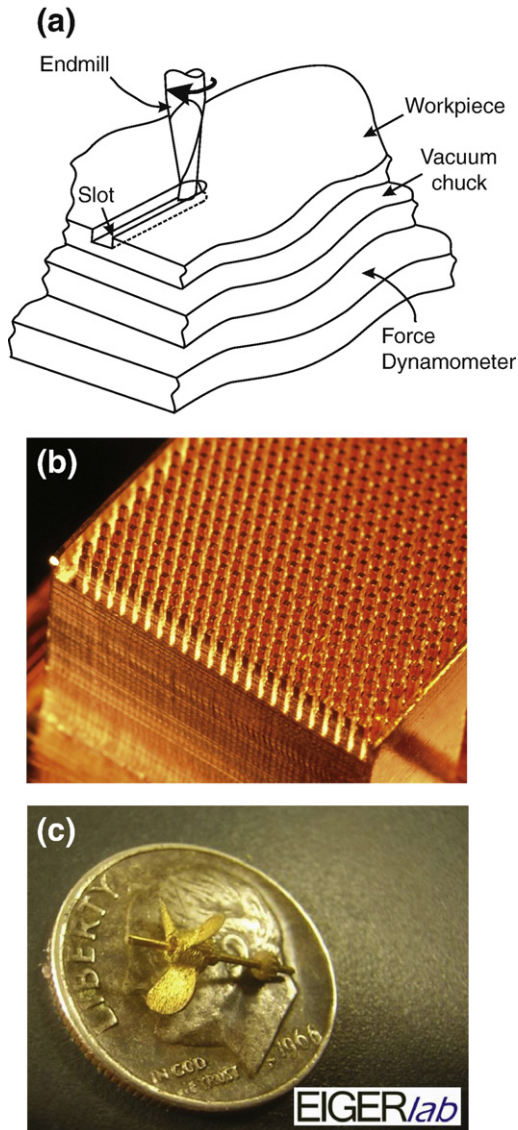


Fig. 1. Micro end milling process and fabricated parts: (a) process schematic, (b) micro-pin heat sink, (c) micro-propeller [30].

micro-propellers, micro-fluidic devices, micro-heat sinks, micro-heat exchangers, and X-ray lithography masks [8,13].

There are several important challenges to overcome when scaling down end mills from conventional to microscopic sizes. The main challenge is that due to their small diameter, micro tools have low flexural stiffness and strength [7,9]. Relatively small cutting forces can significantly bend the tool, negatively affecting the cutting process and potentially causing catastrophic tool failure [7,9]. For example, our empirical evidence shows that cutting forces greater than 10 N will cause a conventional WC end mill with a 300 μm diameter to catastrophically fail. To avoid this, cutting forces must be maintained below a critical value by ensuring that the uncut chip thickness (*i.e.*, the chip load) remains sufficiently small. For many high-strength materials (*e.g.*, steel, titanium, etc.) the maximum allowable uncut chip thickness is on the order of or less than the cutting edge radius (the radius of the forward edge of the tool) which for typical micro end mills is approximately $\sim 1.5 \mu\text{m}$ (Fig. 2). This results in material being removed by a rubbing or burnishing process rather than a cutting process, which accelerates tool wear and produces a poor surface finish [7,9]. Another challenge with smaller tooling is that tool wear has a greater effect on the cutting process [11]. Also, due to the low flexural strength, any chips adhering to the tool (*i.e.*, in the flutes) will eliminate a path for chips to evacuate the cutting zone and result in a spike in the cutting forces, usually leading to tool failure via fracture.

Diamond coatings for micro end mills are promising because of their potential to reduce flute clogging by eliminating adhesion of workpiece material to the tool surface, to reduce the rate of tool wear due to their high hardness, and to reduce the magnitude of cutting forces due to their low coefficient of friction against many materials. Conventional polycrystalline diamond coatings that are currently used to coat macro-scale cutting tools are too thick (2–100 μm) for micro tools because they significantly increase the cutting edge radius, blunting the tool. Thin coatings are needed because the existing cutting edge radius of uncoated tools is already larger than desirable, and further increasing the cutting edge radius will negatively affect the tool's performance. Conventional polycrystalline diamond coatings also generally suffer from poor substrate adhesion, high surface roughness, and high internal stresses [1]. Due to the size of the cutting zone and specifically the uncut chip thickness, continuous polycrystalline diamond coatings, which are typically thicker than at least 2 μm , are too thick for micro tools. Therefore, to minimize the resulting cutting edge radius, thin, fine-grained diamond coatings for micro end mills are investigated here. By achieving high nucleation densities, we are able to grow thin ($< 1 \mu\text{m}$) continuous films. These films are not as thin or fine-grained as NCD, but are at the thinnest and finest-grained limit of MCD films ($< 2 \mu\text{m}$ in terms of both thickness and grain size).

2. Experimental procedure

2.1. Diamond growth

The substrates for diamond growth were 300 μm diameter, two-flute, WC end mills with a shank length of 600 μm . The

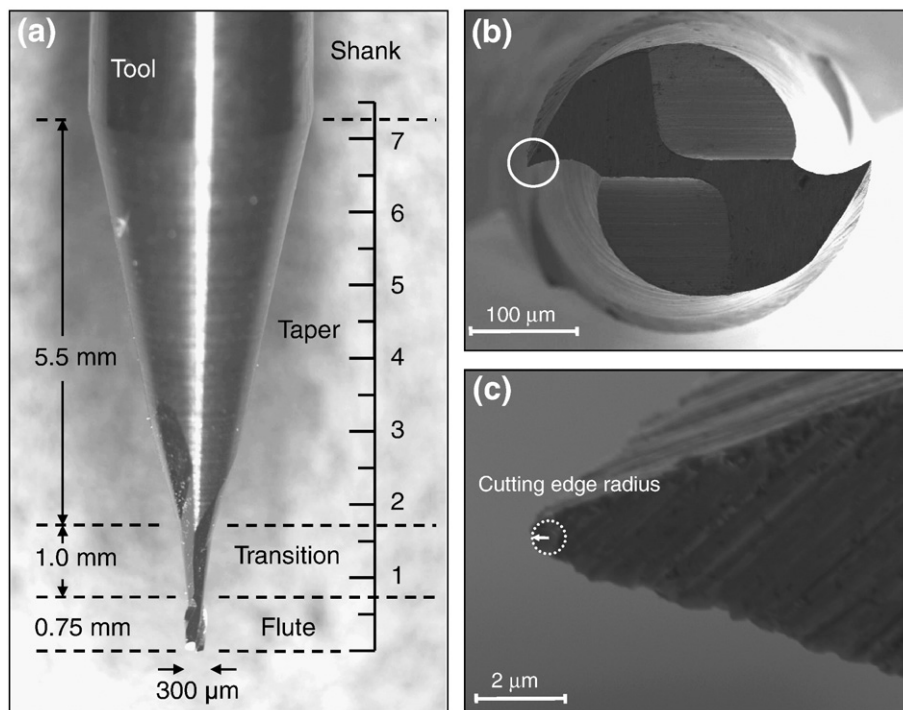


Fig. 2. Tool images: (a) optical image showing all sections of a tool, (b) SEM image of the cutting end of an end mill, and (c) SEM image of a corner of the tool.

tools contained between 6 and 8 wt.% cobalt at the WC grain boundaries. The tools are of a standard, commercially available design supplied by Performance Micro Tool, Inc (Fig. 2). All tools were initially inspected by scanning electron microscope (SEM) and sorted for defects and by diameter, with only defect-free tools used in this study. The circled corner in Fig. 2(b) is magnified for closer examination of wear, breakage, and cutting edge radius. The tools are inspected after each step in the diamond growth process namely etching, seeding, and diamond growth. Table 1 gives diamond film growth conditions that will be discussed in the following sections.

2.1.1. Etching

The 6–8 wt.% Co at the WC grain boundaries increases the ductility of the tool. Removing Co weakens the tool. However, Co must be removed from the surface because it has a negative effect on diamond growth. The catalytic reaction of the growth species with Co enhances precipitation of non-diamond phases. This weakens the bond between the diamond film and substrate, and suppresses diamond growth by limiting nucleation [3]. It also makes growing a thin, continuous film more difficult. Therefore, an etching step is required to selectively etch an optimal amount of Co from the tool surface such that diamond deposition is not affected without weakening the tool significantly. Etching Co from the WC tool surface is a standard step in many other growth processes [2,3,5,6,22–24].

The deleterious effect of Co is illustrated in Fig. 3, which shows an SEM image of a tool where Co suppressed the diamond growth in one region. The corner of the depicted tool was broken after etching, which exposed Co on the fracture surface. A conformal diamond film was grown everywhere except where

the tool was broken and the Co exposed. Clearly, control of the etching step is important to maintain both the tool and coating integrity.

The etching solution was a mixture of HF, HNO₃ and DI water (Table 1). Auger electron spectroscopy, which detects surface chemistry at a depth less than 5 nm, was used to examine the surface concentration of Co after etching. Several tools were etched in different concentrations for different time durations and then examined. The solution concentration and

Table 1
Nominal fine-grained diamond coating growth conditions

Etching	
Acid composition	
50% HF	10 ml
Nitric acid	20 ml
DI water	30 ml
Acid etching time	7 s
Seeding	
Duration of ultrasonic treatment with diamond nanopowder in acetone	15 min
Duration of ultrasonic cleaning with acetone	10 min
Growth	
Tool position below the filament	~3.5 mm
Methane flow	4 sccm (case 1) 6 sccm (case 2)
Hydrogen flow	96 sccm (case 1) 94 sccm (case 2)
Chamber pressure	30 torr
Growth time	45 min (case 1) 30 min (case 2)
Temperature (estimated)	925 °C

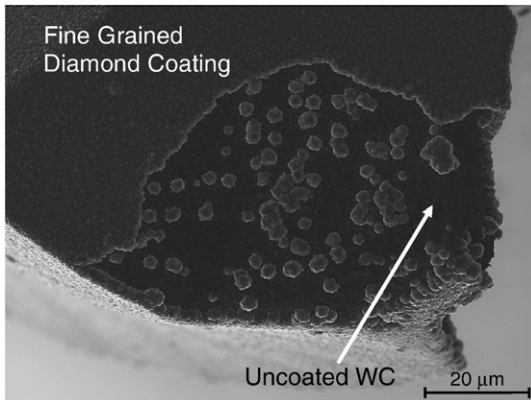


Fig. 3. Scanning electron micrograph of unetched tool corner with suppressed diamond growth.

etching time used in this study was determined from a parametric study to determine the shortest etch time for removing 95% of the Co from the surface.

Since Co is present mostly at the grain boundaries of the WC, etching roughens the tool surface by removing material between the WC grains. This can be seen in Fig. 4, which shows SEM images of the cutting edge of a micro end mill. Figure 4(a) shows an unetched tool and Fig. 4(b) shows the same corner after etching. The surface is somewhat rougher, and grain

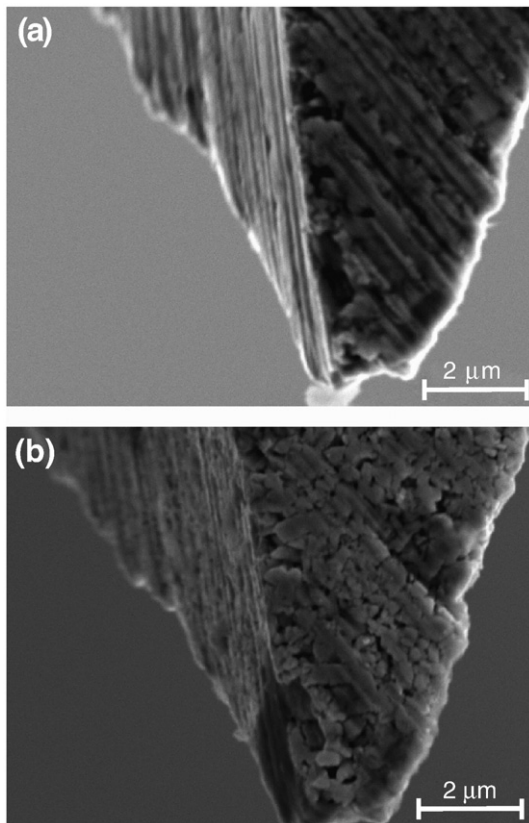


Fig. 4. Scanning electron micrographs of tool corner: (a) before etching, (b) after etching.

boundary etching is apparent. The rougher surface can aid in the adhesion of the coating to the tool by creating locations for the diamond to mechanically ‘anchor’. However, over-etching significantly weakens the tool. Machining tests with uncoated tools etched for various times were conducted to evaluate the tool strength after etching. Tools with etching times longer than 7 s failed faster than tools etched for 7 s. The tools etched for 7 s performed as well as unetched tools. Thus, 7 s of etching is long enough to remove the surface Co, but short enough not to significantly affect tool strength.

During use, the micro end mills have a propensity to fracture in torsion in the transition region between the flute and taper where the flute geometry begins (Fig. 2a), approximately 1 mm from the tool end. As an example, Fig. 5 shows a tool tip that has broken off during machining. Since this region is not used for cutting, it is undesirable to etch this far up the tool. Therefore, a micro-positioner was used to etch only the first 500 μm of the tool to avoid weakening the transition region.

2.1.2. Seeding

After etching, a seeding step is used to increase the nucleation density of the film. It is well known that diamond does not grow easily on most non-diamond substrates, hence nano-diamond powder is used in a standard fashion to help promote the growth process [25]. Seeding is accomplished by using an ultrasonic treatment of the tool in a diamond powder and acetone solution. A nano-diamond (4–10 nm) powder synthesized using the detonation technique [25] is used to make the solution, as it is known to be successful at creating thin, conformal diamond coatings.

Uneven seeding leads to agglomeration of diamond during growth. Therefore, after ultrasonic seeding, we perform an ultrasonic rinsing step in an alcohol solution to ensure uniform seeding without any agglomerations. Figure 6 shows SEM images of tools after deposition. Figure 6(a) shows a tool that was seeded but not rinsed, whereas Fig. 6(b) is a tool that was seeded and rinsed for 5 min. Rinsing greatly reduced the number of agglomerations after deposition, with evidence that increasing the rinse time to 10 min almost eliminates all agglomerations. Rinsing for longer times has no further observable effect.

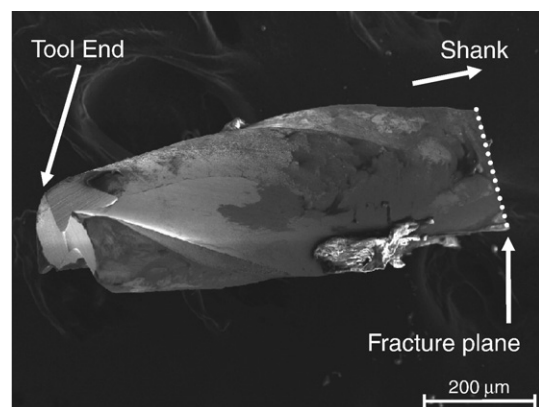


Fig. 5. Side view of broken tool tip.

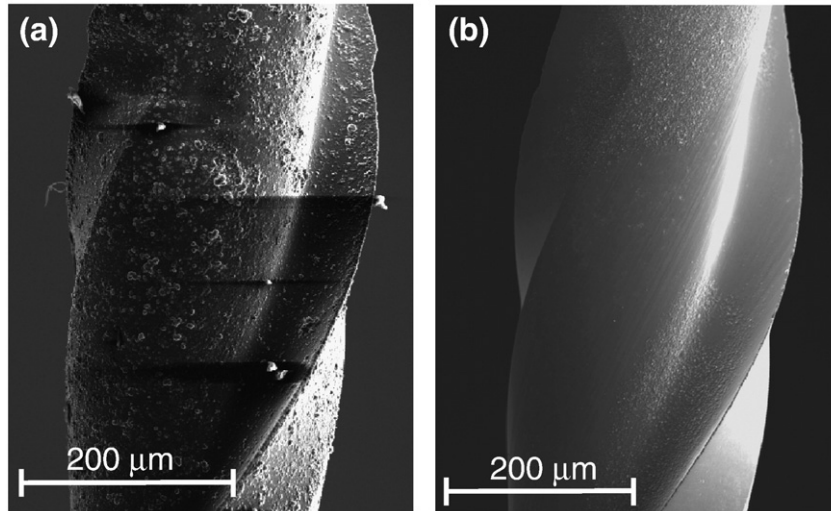


Fig. 6. Scanning electron micrographs of fine-grained diamond coated tools that were seeded and: (a) not rinsed, (b) rinsed for 5 min.

2.1.3. Growth

The seeded tools were coated with the fine-grained diamond film in a hot filament chemical vapor deposition (HFCVD) system (Fig. 7) [26]. The HFCVD system consists of a chamber that is under vacuum (base pressure $\sim 10^{-3}$ torr) where gasses are flowed over a white hot tungsten (W) filament maintained at a temperature of at least 1800 °C.

The tool is mounted in a tool holder and positioned 5 mm below the filament so that it will be radiatively heated by the filament and be within the mean free path of the hydrocarbon radicals produced at the filament. The chamber is then evacuated and maintained at ~ 30 torr during gas flow. A mixture of precursor gases, specifically methane (CH_4) diluted in an excess of hydrogen (H_2), is passed over the filament which is heated to ~ 2000 °C. The hot filament dissociates the H_2 into atomic hydrogen (H°) and CH_4 into hydrocarbon species, (either C_2H_2 or CH_3) [1]. These hydrocarbon species condense on the substrate in the form of graphite and amorphous carbon [1]. The atomic hydrogen etches the non-diamond components faster than they are deposited [1]. The diamond coating grows as the carbon species attach to the seeded diamond nuclei via hydrogen abstraction reaction. The deposition is run long enough to allow

the nuclei to grow together forming a continuous coating. Nucleation density is critical; with greater nucleation density nuclei have a shorter distance to grow before they coalesce, forming a thinner continuous coating. With less nucleation, the nuclei have a greater distance to grow resulting in a thicker coating.

The temperature of the tool is critical for proper diamond deposition. The filaments need to be at least 1800 °C so that H_2 and CH_4 are dissociated and the tool needs to be correctly positioned so that it is at a suitable temperature for diamond growth (~ 925 °C) [1,2,27,28]. There is a large temperature gradient around the filament. Therefore, even a small change in position can greatly affect the tool temperature. After setting the distance between the tool and filament, the tool temperature is controlled by adjusting the power of the filament. To ensure a proper coating, the tool temperature is monitored by a two color pyrometer that operates at wavelengths where the hydrogen plasma and quartz window are transparent. The pyrometer is used to measure a relative temperature at the very tip of the tool to aid in growth reproducibility rather than measuring an actual temperature. The spot size of the pyrometer is slightly larger than the tool which significantly increases the error of the temperature reading. The tool is highly reflective which also creates error in the temperature reading. However, when correctly used the pyrometer helps us determine the relative tool temperature within 10 K.

Temperature variations on the tool result in a significant change in the coating properties. When the temperature is too low, there is reduced diamond growth, and the coating is not continuous. When the temperature is too hot, more graphite is formed and diamond grains are not easily identified. At the correct temperature, approximately 925 °C, diamond grains are formed consistently and continuously over the entire tool tip.

2.2. Micro end milling

2.2.1. Apparatus

Figure 8 illustrates the geometry for the machining experiments. A high-speed spindle (NSK-HES500, Japan)

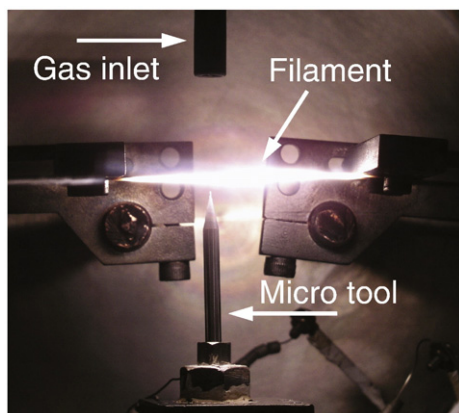


Fig. 7. Image of hot filament chemical vapor deposition (HFCVD) chamber.

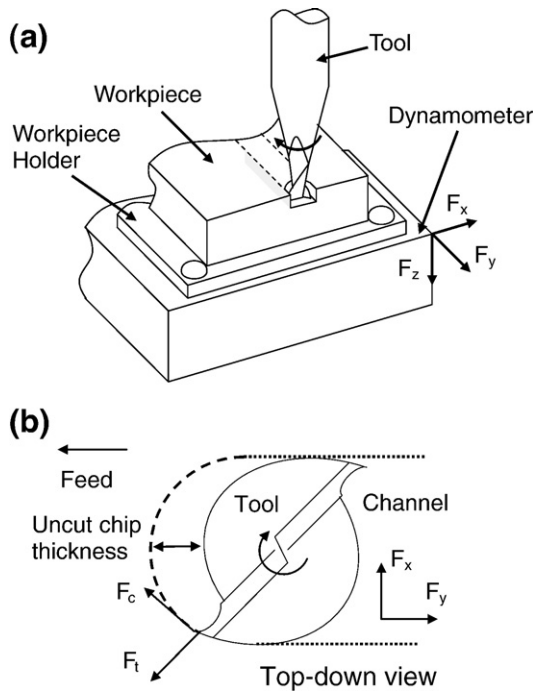


Fig. 8. Schematic of micro end milling (a) 3D view of experiment, and (b) end view of cutting process.

with electric drive and ceramic bearings is mounted to the spindle of a CNC milling machine (HAAS TM-1, Oxnard, CA). The CNC mill positions and translates the tool with respect to the workpiece to achieve the desired depth of cut and feed rate. The high-speed spindle (5000–50,000 rpm) is operated at 40,000 rpm for all of the experiments.

The chip load describes the maximum uncut chip thickness (Fig. 8b): *i.e.*, the distance the tool translates per rotation of the tool divided by the number of cutting flutes. The chip load is controlled by the feed rate because the spindle speed is held constant throughout these tests. We used a feed rate of 500 mm/min., thus the chip load was 6.25 μm per tooth.

The workpiece is mounted on a force dynamometer (Kistler 9256C2 Winterthur, Switzerland) that can measure the cutting forces dynamically in the x , y , and z axes. The absolute magnitude of the dynamic force data has an unspecified bias associated with it because the cutting frequency is close to the natural frequency of the dynamometer. The natural frequency of the dynamometer with the workpiece mounted is approximately 4 kHz and the forcing frequency of a two-flute end mill rotating at 40,000 rpm is 1.3 kHz. Therefore, workpieces of identical mass are always used so that the data between different cutting conditions can be compared. Several tests were conducted to determine that the machining conditions were under stable conditions. The x and y data are used to calculate the thrust (*i.e.*, radial) force, F_t , and main cutting (*i.e.*, tangential) force, F_c . A humidity control system is used to maintain a constant relative humidity. The humidity system uses two nozzles to flow humid air across the tool tip to ensure a constant relative humidity of approximately 85% at the tool tip.

Table 2
Nominal machining conditions

Workpiece material	6061-T6 aluminum
Room temperature	$\sim 23^\circ\text{C}$
Relative humidity	$\sim 85\%$
Tool (end mill)	
Material	0.4 μm grain carbide
Diameter	304.8 μm (0.012 in.)
Flutes	2
Helix	30°
Spindle speed	40,000 \pm 500 rpm
Feed rate	500 mm/min
Feed	12.5 $\mu\text{m}/\text{rev}$
Chip load	6.25 $\mu\text{m}/\text{tooth}$
Coolant	None
Depth of cut	100 \pm 5 μm

2.2.2. Machining procedure

The machining conditions used are shown in Table 2. The tests consist of machining a single full-width channel 5 mm long and 100 μm deep, in 6061-T6 aluminum, without using a cutting fluid. The workpiece is mounted on the dynamometer before preparing the surface. The workpiece surface is prepared by facing with a one inch end mill to ensure flatness to within 3 μm , and then polished to reduce the surface roughness. Each tool is fixtured in the high-speed spindle and then aligned to the workpiece using an optical magnification system. The alignment uncertainty is ± 5 μm in the z -axis, which corresponds to the uncertainty in the depth of cut. LabView software and

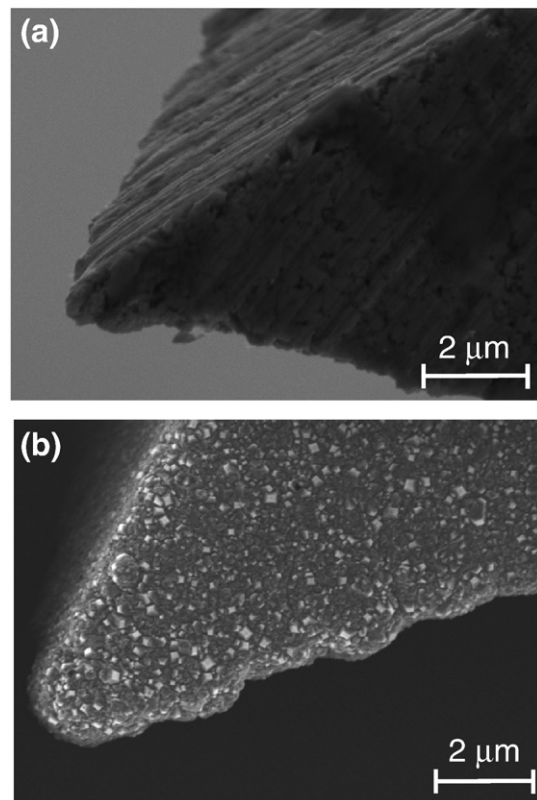


Fig. 9. SEM images showing the cutting edge radius of unused: (a) uncoated tool, and (b) fine-grained diamond coated tool.

National Instruments data acquisition hardware are used to record the force data at a rate of 60 kHz. Both uncoated and coated tools were run in the same test batch to ensure compatibility between tests.

3. Results and discussion

3.1. Fine-grained diamond coating properties

Several micro end mills were successfully coated with diamond. Figure 9 shows two SEM micrographs of an unused new tool before and after diamond deposition. Coatings had variations in thickness, grain size and sp^2/sp^3 ratios. Some variations were random and a result of developing a reproducible procedure, other variations resulted from deliberately changing growth parameters in an attempt to optimize the resulting coating.

First, a coating procedure was developed so that a reproducible diamond coating was obtained. Several tools were grown with the initial conditions of 4% methane (Fig. 10a). To achieve a continuous film, the film needed to be grown to a thickness of 0.5–1 μm , resulting in grain sizes estimated to be 0.1–1 μm . These first tools were used to evaluate the difference in performance between coated and uncoated tools. These coatings machined better than the uncoated tools and survived for several channels.

To further improve tool machinability, growth parameters were changed to optimize the coating. The growth conditions

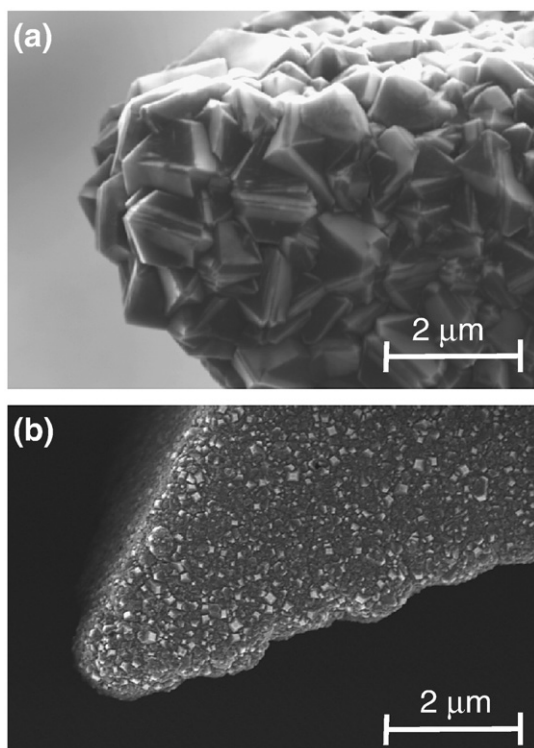


Fig. 10. SEM images showing grain size and faceting for: (a) MCD with average grain size of 1–3 μm and (b) fine-grained diamond coatings with average grain size of 30–300 nm.

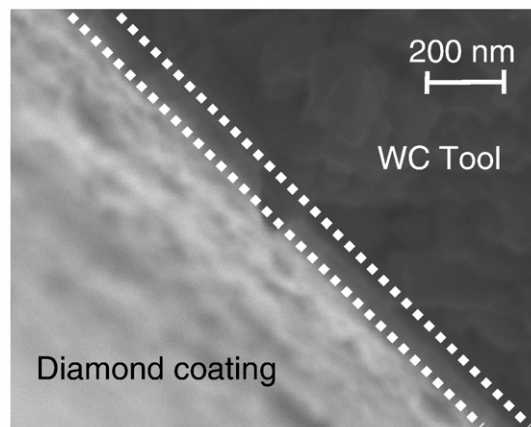


Fig. 11. SEM image showing the thinnest fine-grained diamond coating achieved.

were changed by increasing the methane percentage from 4% to 6%. This allows continuous films to be grown as thin 170 nm (Fig. 11). Films grown under conditions with thicknesses from 170–500 nm had grain sizes ranging from 30–300 nm.

Figure 12 shows the Raman spectrum of a typical fine-grained diamond film deposited with 4% and 6% CH_4 respectively. The diamond film grown with 4% CH_4 shows presence of a sharp peak at 1332 cm^{-1} and no observable peak at 1580 cm^{-1} indicating good quality microcrystalline diamond with negligible amount of non-diamond phase. Whereas, Raman spectrum of diamond film grown with 6% CH_4 has a relatively distinct broad 1332 cm^{-1} peak indicating fine-grained diamond and a big hump at 1580 cm^{-1} indicating presence of amorphous carbon at the grain boundaries due to increased grain boundary fraction. Additionally, the small shoulder at 1140 cm^{-1} is believed to be due to the presence of *trans*-polyacetylene more commonly observed in fine-grained diamond films. In short, from the Raman spectra, it is clear that the diamond film grown with 4% CH_4 is good quality microcrystalline diamond, with average estimated grain size 0.1–1 μm , and that grown with 6% CH_4 is fine-grained diamond, with average grain size 30–300 nm, with amorphous carbon at the grain boundaries. The

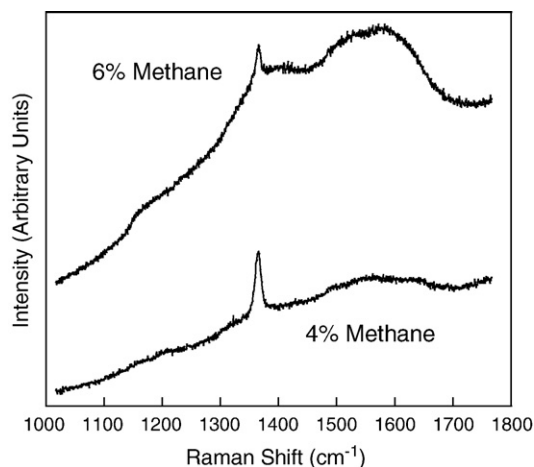


Fig. 12. Visible Raman spectrum, using a 532 nm YAG laser, of typical fine-grained diamond (6% CH_4) and microcrystalline diamond (4% CH_4) films grown using HFCVD.

grain sizes are estimated from topographic SEM images. We are currently working on calculating grain size from a rigorous systematic cross sectional process, which, we feel, will result in grain size averages which are less than the current estimates. The decrease in the diamond grain size with increase in methane concentration is clearly evident from the SEM micrographs shown in Fig. 10(a) and (b) respectively.

The 6% methane coatings delaminated immediately during machining tests, while the 4% methane coatings did not delaminate during machining tests. The poorer performance of the 6% films could be due to poor substrate adhesion, higher intrinsic film stress or lower films strength. These factors are the subject of current study. Tools that were subsequently subjected to additional testing by machining more channels eventually delaminated. The higher methane content results in thinner fine-grained diamond coatings that have a tendency to delaminate. The 4% methane mixture results in larger grain size and coating thickness, however these coatings resulted in less delamination. There are large shear forces on the interface between the coating and tool when machining. The coatings with less adhesion delaminated and failed due to these large forces. Therefore, our future goal is to reduce the grain size (*i.e.*, diamond film thickness) while still promoting coating-substrate adhesion. The following machining results for coated tools are from experiments conducted with the 4% methane coatings.

3.2. Fine-grained diamond machining performance

3.2.1. Cutting forces

Applying a fine-grained diamond coating reduces the thrust and main cutting forces by approximately 90% and 75%, respectively compared with uncoated tools, for the machining conditions used in this study (Fig. 13). There is also a change in the ratio of thrust force to cutting force. The uncoated tool has a much larger thrust force compared to cutting force, which is representative of a rubbing or plowing action rather than cutting. The coated tool has cutting and thrust forces which are equal within the uncertainty. This force ratio is typical of cutting

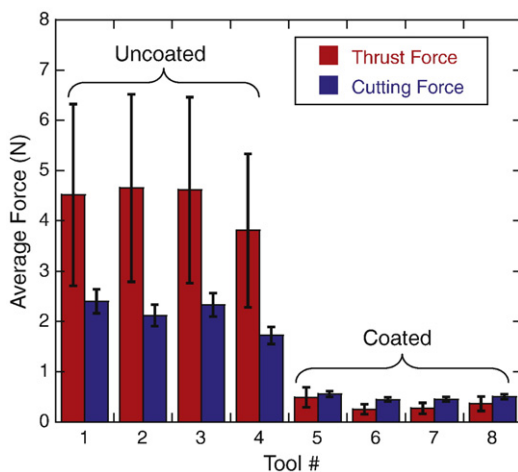


Fig. 13. Comparison of average cutting forces for uncoated and fine-grained diamond coated tools.

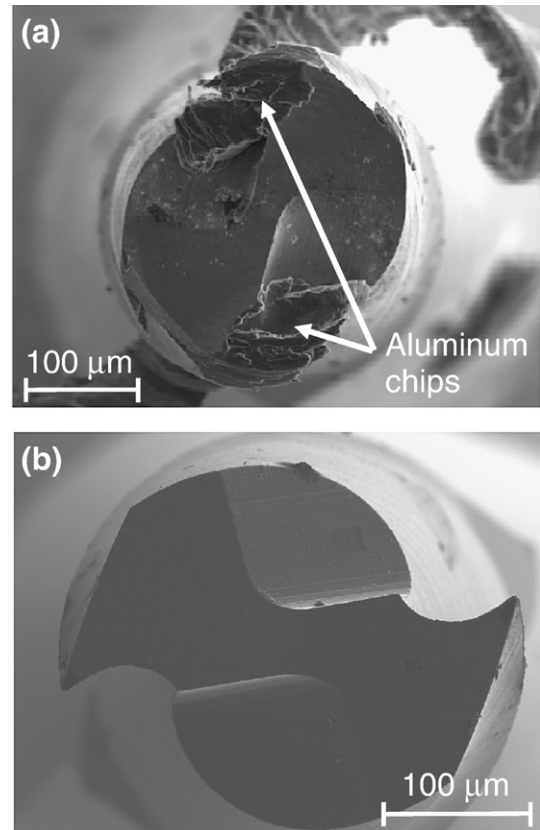


Fig. 14. SEM images showing aluminum adhesion after machining: (a) uncoated tool, and (b) fine-grained diamond coated tool.

with a chip load that is similar in magnitude with the cutting edge radius [9,11]. The force ratio of unity for the coated tools also suggest that plastic deformation in the primary shear zone is more dominant than for the uncoated tool where friction along the rake face and elastic deformation of the unmachined material make a significant contribution [9,11].

3.2.2. Chip adhesion

After machining, the uncoated and coated tools were examined by SEM. The uncoated tools had large chips adhering to them (Fig. 14a). Energy dispersive spectrometry (EDS) was used to confirm that the chips were aluminum. The uncoated tools always showed wear in the form of broken cutting tips. The fine-grained diamond coated tools showed no adhered aluminum and no wear as long as the coating remained intact (Fig. 14b). However, if the coating delaminated from the tool, the tool showed adhered chips and wear, but only where there was exposed WC. This is evidence that the chips encounter less resistance in traveling up the flutes and away from the cutting zone on fine-grained diamond coated tools, which results in lower forces acting on the tool, which is indeed what is observed.

3.2.3. Workpiece surface roughness and burr formation

The bottoms of the machined channels were examined to further evaluate the tools' performance. The topography of the bottom of all the channels machined by the uncoated tool was

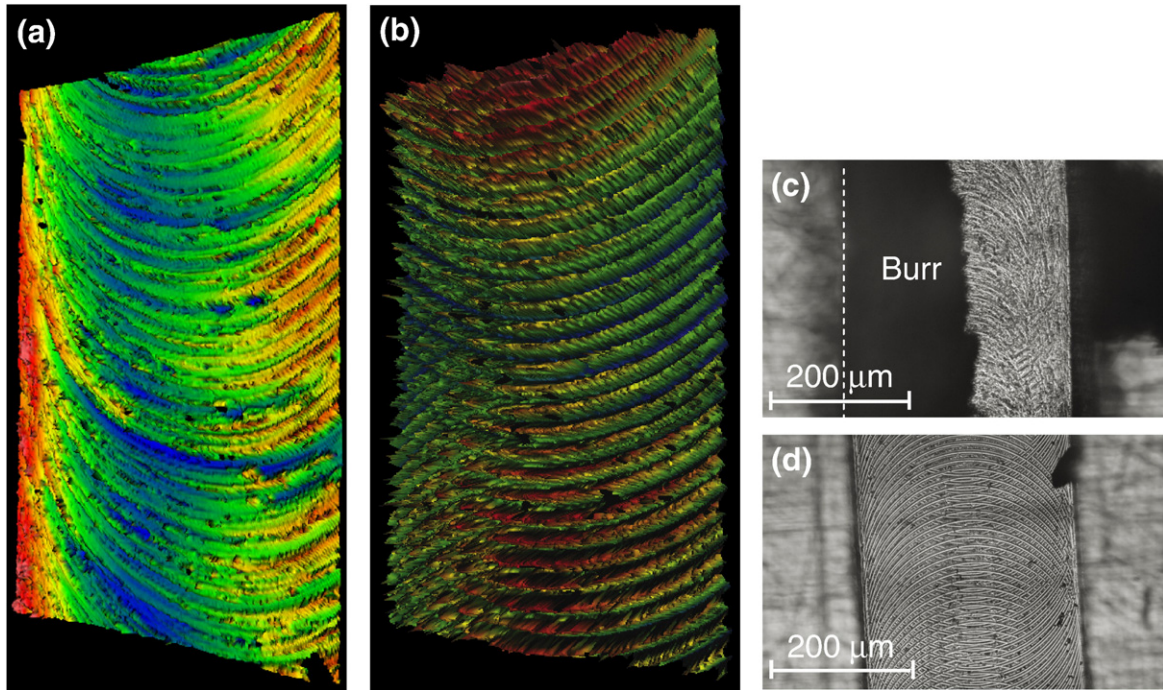


Fig. 15. Comparison of the surface roughness at the bottom of 6061-T6 aluminum channels machined under the nominal operating conditions: white light interferometer images of (a) uncoated tool, (b) fine-grained diamond coated tool; optical micrographs of (c) uncoated tool, and (d) fine-grained diamond coated tool.

not uniform (Fig. 15a). The non-uniform surface topography suggests a significant amount of heat generation and smearing throughout the cutting process. This indicates that the tool, or material adhered to the tool, is rubbing the workpiece surface. Higher temperatures in the cutting zone due to friction along the tool surface will increase the propensity of workpiece material to adhere to the tool resulting in smearing. On the other hand, the fine-grained diamond coated tool typically made uniformly periodic surface features (Fig. 15b), as seen in a typical macro-scale end milling.

Analysis of the channels using white light interferometry revealed that the diamond coated tool produced a smoother channel than the uncoated tool (Fig. 15c–d). For the uncoated tool the mean roughness $R_a=350$ nm and RMS roughness $R_q=450$ nm whereas for the diamond coated tool $R_a=325$ nm and $R_q=400$ nm. Cutting marks can be seen in the channel machined with the uncoated tool (Fig. 15c), although these marks appear to have been smeared out compared with the features generated by the coated tool (Fig. 15d). The coated tool cuts much more cleanly leaving a standard, repeatable surface finish in all channels. In contrast, the surface finish produced by the uncoated tools under the current operating conditions varies within a single channel and between subsequent cuts (*i.e.*, channels). The smearing action can occasionally produce surfaces smoother than those generated by a fine-grained diamond coated tool. However, on average they are still rougher as indicated by the R_a and R_q measurements reported above. The coated tools can produce surfaces rougher than the uncoated tool because the cutting tips stay intact, the aluminum does not adhere to the diamond coating, and the cutting temperature is lower, resulting in better defined valleys and peaks being gen-

erated (Fig. 15b). The well-defined and repeatable surface generated by the diamond coated tool is desirable because it is predictable.

The uncoated tools frequently produce significant burring (Fig. 15c). For the cutting parameters used in this study there is burring on the top edges of the channel as well as a burr that obstructs half of the channel width and running the entire length. The top-edge burr is due to a higher friction coefficient, adhesion, and a greater amount of heat generated during the cutting operation. The result is that rubbing and plowing occur at the cutting edge, which pushes a significant amount of material in front of the tool and out of the channel, instead of directing the material along the rake face and into the flutes. The coated tool does not produce any observable burring (Fig. 15d), again suggesting that the cutting process is occurring at significantly lower temperature, with less friction and adhesion on the tool surfaces. This enables fracture at the chip root which creates a chip that can flow up along the flutes, which is then removed from the cutting zone.

The uncoated tools also produce larger continuous chips of various sizes, while the coated tools make shorter, more uniform chips. The continuous chips are unusual for an interrupted cutting process such as end milling because a cutting edge is only engaged with the workpiece for 180 degrees of rotation. The continuous chips are likely generated by the uncoated tool because a newly generated chip adheres to the flute surface and is only moved after a newly generated chip is pushed into it, welding them together. This mechanism results in higher cutting forces because a chip that has just been removed from the workpiece must also dislodge a chip adhering to the flute that was generated on the previous tool rotation. These results were

verified by using a high-speed video camera to observe the tools while cutting. It was clearly observed that the coated tool cut with less burring producing many small uniform chips, while the uncoated tool created a large amount of burring producing only a few long continuous chips.

4. Conclusions

This preliminary study has shown that it is possible to coat WC micro tools (300 μm diameter) with fine-grained diamond, with average grain size 30–300 nm, and that the fine-grained diamond coating dramatically improves the cutting performance of the tools when machining aluminum without any cutting fluid. The fine-grained diamond coating reduced the thrust and main cutting forces by approximately 90% and 75%, respectively compared with uncoated tools, when machining 6061-T6 aluminum. Further studies need to be performed to better evaluate and understand the improvement in performance when machining a variety of metals. Humidity tests will also be important, since diamond's coefficient of friction is dependent on humidity [29].

By altering the gas chemistry (increasing CH_4 from 4% to 6%) the thickness and grain size of the coating was reduced. Reducing coating thickness is important as tool diameter decreases to maintain the cutting edge radius. However, the change in gas chemistry deleteriously changed the carbon bonding, producing more sp^2 -bonded carbon, weakening the coating's strength. Delamination also occurred far more readily. Further optimization of growth conditions to reduce grain size while maintaining the films strength and continuity is readily feasible.

Further work needs to be done to improve the adherence of the coating to the tool. Delamination of the coating typically occurs after several minutes of machining. Delamination is sudden and can clearly be seen by a sharp increase in forces and the production of burrs. After delamination, the tool looks similar to an uncoated tool with worn and/or broken tool corners and adhered workpiece material. It is not clear if the corner of the tool breaks and causes delamination, or if the tool delaminates and the corner breaks due to wear. We are currently investigating a range of surface preparation methods before deposition to increase the coating's adherence to the tool.

Preliminary results show that fine-grained diamond coatings can significantly improve the performance of micro tools. As these coatings are further developed, achievable micro-machining tolerances will be improved and may even assist in the successful use of even smaller tools. This will allow micro-machining to become a more important and environmentally benign tool for manufacturing micro- and meso-scale parts.

Nomenclature

F	force, N
R_a	average surface roughness, μm
R_q	RMS surface roughness, μm
MCD	microcrystalline diamond
NCD	nanocrystalline diamond
WC	tungsten carbide

Subscript

x,y,z	global coordinate direction
c	main (tangential) cutting force with respect to cutting edge
t	thrust (radial) cutting force with respect to cutting edge

Acknowledgements

Support of this work by the Graduate School of the University of Wisconsin-Madison with an Industrial and Economic Development Research Grant is gratefully acknowledged. The authors would like to thank Mr. Yongho Jeon and Derek Wissmiller for their invaluable assistance with micro end milling experiments and Dave Burton from Performance Micro Tool for supplying micro end mills.

References

- [1] C. Chang, Y. Liao, G.Z. Wang, Y.R. Ma, R.C. Fang (Eds.), *Crystal Growth Technology*, Springer, Heidelberg, 2003, p. 93, 4 CVD Diamond Growth.
- [2] M.J. Jackson, M.D.H. Gill, H. Sein, W. Ahmed, *Proceedings of IMechE Part L: Journal of Materials: Design and Applications*, vol. 217, 2003, p. 77.
- [3] H. Sein, W. Ahmed, M. Jackson, R. Woodward, R. Polini, *Thin Solid Films* 447-448 (2004) 455.
- [4] R.A. Hay (Ed.), *Ceramic Cutting Tools, The New Diamond Technology and its Application to Cutting Tools*, vol. 11, William Andrew Publishing/Noyes, Norwich, NY, 1994, p. 305.
- [5] J. Schwarz, K. Meteva, A. Grigat, A. Schubnov, S. Metev, F. Vollersten, *Diamond Relat. Mater.* 14 (2005) 302.
- [6] H.Y. Ueng, C.T. Guo, *Appl. Surf. Sci.* 249 (2005) 246.
- [7] A. Kobayashi, *Industrial Diamond Review* (2005) 28.
- [8] F. Bruno, C. Friedrich, R.O. Warrington, *IEEE Transactions on Industrial Electronics* 42 (1995) 423.
- [9] X. Liu, R.E. Devor, S.G. Kapoor, K.F. Ehmman, *J. Manuf. Sci. Eng.* 126 (2004) 666.
- [10] R.E. Williams, Y. Huang, S. Melkote, B. Kinsey, W. Sun, D. Yao, *International Mechanical Engineering Congress and Exposition*, 2005, ASME, Orlando, FL, November 5-11, 2005, IMECE2005-79889.
- [11] J. Chae, S.S. Park, T. Freiheit, *Int. J. Mach. Tools Manuf.* 46 (2006) 313.
- [12] B.N. Damazo, M.A. Davies, B.S. Dutterer, M.D. Kennedy, *1st International Conference and General Meeting of the European Society of Precision Engineering and Nanotechnology*, Bremen, May 31 - June 4 1999, p. 322.
- [13] C. Friedrich, P. Coane, J. Goettert, N. Gopinathin, *Precis. Eng.* 22 (1998) 164.
- [14] C.-J. Kim, M. Bono, J. Ni, *SME Technical Paper MR02-159*, 2002, p. 1.
- [15] K. Lee, D.A. Dornfeld, *SME Technical Paper MR02-202*, 2002, p. 353.
- [16] J.R.S. Prakash, M. Rahman, K.A. Senthil, S.C. Lim, *Chinese J. Mech. Eng.* 15 (supplement) (2002) 115.
- [17] T. Schaller, L. Bohn, J. Mayer, K. Schubert, *Precision Engineering* 23 (1999) 229.
- [18] M. Takacs, B. Vero, *Materials Science Forum* 414-415 (2003) 337.
- [19] I. Tansel, M. Trujillo, A. Nedbouyan, C. Velez, W.Y. Bao, T. Arkan T.B., *Int. J. Mach. Tools Manuf.* 38 (1998) 1419.
- [20] M.P. Vogler, X. Liu, S.G. Kapoor, R.E. Devor, K.F. Ehmman, *SME Technical Paper MS02-181*, 2002, p. 1.
- [21] K. Isomura, M. Murayama, H. Yamaguchi, N. Ijichi, H. Asakura, N. Saji, O. Shiga, K. Takahashi, S. Tanaka, T. Genda, M. Esashi, *ASME Turbo Expo*, Amsterdam, Netherlands, 2002, p. 1127.
- [22] M.J. Jackson, L.J. Hyde, W. Ahmed, H. Sein, R.P. Flaxman, *J. Mater. Eng. Perform.* 13 (2004) 421.
- [23] F.-X. Lu, W.-Z. Tang, J.-Q. Miao, L.-F. He, C.-M. Li, G.-C. Chen, *Diamond Relat. Mater.* 15 (2006) 2039.
- [24] V. Vohra, S.A. Catledge, Y.K. Vohra, *Mechanical Properties of Nanostructured Materials and Nanocomposites Symposium*, MRS, Boston, MA, Dec. 1-5 2003, p. 277.

- [25] A.V. Sumant, P.U.P.A. Gilbert, D.S. Grierson, A.R. Konicek, M. Abrecht, J.E. Butler, T. Feygelson, S.S. Rotter, R.W. Carpick, *Diamond Relat. Mater.* 16 (2007) 718.
- [26] H.Y. Yap, B. Ramaker, A.V. Sumant, R.W. Carpick, *Diamond Relat. Mater.* 15 (2006) 1622.
- [27] M.J. Jackson, G.M. Robinson, W. Ahmed, H. Sein, A.N. Jones, N. Ali, E. Titus, Q.H. Fan, J. Gracio, *J. Mater. Eng. Perform.* 14 (2005) 163.
- [28] P.W. May, J.N. Harvey, J.A. Smith, Y.A. Mankelevich, *J. Appl. Phys.* 99 (2006) 104907.
- [29] E. Liu, Y.F. Ding, L. Li, B. Blanpain, J.P. Celis, *Tribology International* 40 (2007) 216.
- [30] EIGERlab, personal communication, 2006.